
Time-Variant Variational Transfer for Value Functions

Giuseppe Canonaco*

Politecnico di Milano, Milan, Italy
giuseppe.canonaco@polimi.it

Andrea Soprani*

Politecnico di Milano, Milan, Italy
andrea.soprani96@gmail.com

Manuel Roveri

Politecnico di Milano, Milan, Italy
manuel.roveri@polimi.it

Marcello Restelli

Politecnico di Milano, Milan, Italy
marcello.restelli@polimi.it

Abstract

In most of the transfer learning approaches to reinforcement learning (RL) the distribution over the tasks is assumed to be stationary. Therefore, the target and source tasks are i.i.d. samples of the same distribution. In the context of this work, we consider the problem of transferring value functions through a variational method when the distribution that generates the tasks is time-variant, proposing a solution that leverages this temporal structure inherent in the task generating process. Furthermore, by means of a finite-sample analysis, the previously mentioned solution is theoretically compared to its time-invariant version. Finally, we will provide an experimental evaluation of the proposed technique with three distinct temporal dynamics in three different RL environments.

1 Introduction

Reinforcement learning (RL) techniques [32] are becoming increasingly effective in dealing with complex problems [39, 31, 27] at the cost of requiring a huge amount of experience to achieve these impressive results. Therefore, a desirable feature for RL algorithms is sample efficiency, which could be achieved, among all other alternatives, through transfer learning (TL) [34, 18]. TL allows an RL algorithm to reuse knowledge coming from a set of already solved tasks in order to speed up the learning phase of new ones. Depending on what kind of knowledge representation is being transferred, we have different TL algorithms in the related literature. Therefore, in order to perform the transfer, we may have algorithms leveraging policies or options [9, 17], samples [33, 20, 38, 36], features [2, 21], value-functions [35, 37] or parameters [15, 1, 26, 8].

In the classical TL setting, the source and target tasks usually come from the same distribution, hence it would be sensible to use the Bayesian framework to iteratively refine the prior knowledge coming from the source tasks as more evidence from the target is collected. Following this rationale, in [40], under the assumption that the tasks share similarities in their Markov Decision Process (MDP) [29] representation, a hierarchical Bayesian solution is proposed, whose main drawback lies in the need to solve an auxiliary MDP in order to perform actions on the task currently faced. Another methodology, along this line of research, has been developed in [19], which still leverages hierarchical Bayesian models, but this time assuming the tasks share commonalities through their value functions. Furthermore, in [6], a Bayesian framework able to adapt optimal policies to variations of the task dynamics is developed. They use a latent variable, which, together with the state-action couple, entirely describes the system dynamics. The uncertainty over the latent variable is modeled independently of the uncertainty over the state. This limitation is overcome in the extension

*equal contribution

to their framework proposed in [15]. In [28] another extension to [6] is proposed, which accounts for multiple variation factors that potentially also come from the reward function. A more general and efficient approach is instead developed in [37], which iteratively refines the distribution over optimal value functions by means of a variational procedure as more experience from the target task is collected.

In real-world applications, the system to be controlled by an agent is very likely to evolve with time. Therefore, in the task generating process of a family of similar tasks, there may be an underlying temporal dynamic to consider. Temporal dynamics are usually not considered in the related TL literature. For this reason, in this paper, we will extend the work developed in [37] in order to take into account a time-variant distribution inherent to the task generating process. We will, then, provide a theoretical comparison between our solution and the time-invariant approach of [37]. Finally, we will provide an experimental comparison of the two approaches in three different RL environments with three distinct temporal dynamics.

2 Preliminaries

In this section, we describe the setting introduced in [37] by adding a time-variant distribution over the tasks. We will start with basic RL concepts and some notation in Section 2.1, and we will conclude with the variational approach to transfer in Section 2.2.

2.1 Reinforcement Learning Background

Let us consider a time-variant distribution \mathcal{D}_t over tasks. We model each task \mathcal{M}_t coming from \mathcal{D}_t as a discounted Markov Decision Process (MDP) [29], which is defined as a tuple $\mathcal{M}_t = \{\mathcal{S}, \mathcal{A}, \mathcal{P}_t, \mathcal{R}_t, p_0, \gamma\}$. \mathcal{S} and \mathcal{A} represent the state space and the action space, respectively. \mathcal{P}_t is the Markovian transition function, where $\mathcal{P}_t(s'|s, a)$ is the transition density from state s to state s' given that the action a is executed on the environment. $\mathcal{R}_t : \mathcal{S} \times \mathcal{A} \rightarrow \mathbb{R}$ is the reward function, assumed to be uniformly bounded by a constant $R_{max} > 0$. p_0 and $\gamma \in [0, 1)$ are the initial state distribution and the discount factor, respectively. Therefore, for each task t our goal is to find a deterministic policy, $\pi_t : \mathcal{S} \rightarrow \mathcal{A}$, maximizing the long-term return over a possibly infinite horizon. In other words, this means being able to get $\pi_t^* \in \arg \max_{\pi} J_t(\pi)$, where $J_t(\pi) = \mathbb{E}_{\mathcal{M}_t, \pi}[\sum_{h=0}^{\infty} \gamma^h \mathcal{R}_t(s_h, a_h)]$. The optimal policy π_t^* is a greedy policy w.r.t. the optimal value function, i.e., $\pi_t^*(s) = \arg \max_a Q_t^*(s, a)$ for all s , where $Q_t^*(s, a)$ is defined as the expected return obtained by taking action a in state s and then following the optimal policy afterward. From now on, for the sake of readability, we will drop the t subscript whenever this does not imply ambiguity.

In this context, we focus on a set of parametrized value functions, $\mathcal{Q} = \{Q_{\theta} : \mathcal{S} \times \mathcal{A} \rightarrow \mathbb{R} | \theta \in \mathbb{R}^p\}$, also called Q -functions. We assume that each $Q_{\theta} \in \mathcal{Q}$ is uniformly bounded by $\frac{R_{max}}{1-\gamma}$. An optimal Q -function is also the fixed point of the optimal Bellman operator [29], which is defined as follows: $TQ_{\theta}(s, a) = \mathcal{R}(s, a) + \gamma \mathbb{E}_{s' \sim \mathcal{P}}[\max_{a'} Q_{\theta}(s', a')]$. Therefore, a measure of optimality for a value function during learning is its Bellman error, defined as $B_{\theta} = TQ_{\theta} - Q_{\theta}$. Of course, if $B_{\theta}(s, a) = 0 \forall (s, a) \in \mathcal{S} \times \mathcal{A}$, then Q_{θ} is optimal, which implies that minimizing the squared Bellman error, $\|B_{\theta}\|_{\nu}^2$, is a good objective for learning (ν is the distribution over $\mathcal{S} \times \mathcal{A}$, assumed to exist). In practice, the Bellman error is not used, since it requires two independent samples of the next state s' for each couple (s, a) [22, 32]. For this reason, usually, the Bellman error is replaced by the Temporal Difference (TD) error $b(\theta)$, which corresponds to an approximation of the former using one sample $\langle s_h, a_h, r_h, s_{h+1} \rangle$, so $b_h(\theta) = r_h + \gamma \max_{a'} Q_{\theta}(s_{h+1}, a') - Q_{\theta}(s_h, a_h)$. Therefore, given a set $D = \langle s_h, a_h, r_h, s_{h+1} \rangle_{h=1}^N$ the squared TD error is $\|B_{\theta}\|_D^2 = \frac{1}{N} \sum_{h=1}^N b_h(\theta)^2$.

2.2 Variational Transfer of Value Functions

In the context described above, an optimal solution to an RL problem is a greedy policy w.r.t. an optimal value function that is parameterized by a vector of weights θ . Therefore, we can safely consider a distribution over optimal weights $p(\theta)$ instead of the distribution \mathcal{D} over tasks since the latter induces a distribution over optimal Q -functions [37]. Now, given a prior on the weights $p(\theta)$ and a dataset $D = \langle s_h, a_h, r_h, s_{h+1} \rangle_{h=1}^N$, the optimal Gibbs posterior that minimizes an oracle upper

bound on the expected loss is known to be [4]:

$$q(\theta) = \frac{e^{-\Psi \|B_\theta\|_D^2} p(\theta)}{\int e^{-\Psi \|B_{\theta'}\|_D^2} p(\theta') d\theta'}, \quad (1)$$

where $\Psi > 0$, which will be set to $\psi^{-1}N$, for some constant $\psi > 0$ as in [37]. It is worth noting that q becomes a Bayesian posterior every time $e^{-\Psi \|B_\theta\|_D^2}$ can be interpreted as the likelihood of D . Since the integral at the denominator of Equation (1) is intractable, a variational approximation through a parametrized family of posteriors q_ξ , such that $\xi \in \Xi$, is proposed. In this way, it is sufficient to find ξ^* such that q_{ξ^*} minimizes the Kullback-Leibler (KL) divergence w.r.t. the Gibbs posterior q , which is equivalent to minimizing the (negative) evidence lower bound (ELBO) [3]:

$$\min_{\xi \in \Xi} \mathcal{L}(\xi) = \min_{\xi \in \Xi} \left\{ \mathbb{E}_{\theta \sim q_\xi} [\|B_\theta\|_D^2] + \frac{\psi}{N} D_{KL}(q_\xi(\theta) \| p(\theta)) \right\}. \quad (2)$$

Algorithm 1 Variational Transfer

- 1: **Input:** Target task \mathcal{M}_t , source weights Θ_s
 - 2: Estimate prior $p(\theta)$ from Θ_s
 - 3: Initialize parameters: $\xi \leftarrow \arg \min_{\xi \in \Xi} D_{KL}(q_\xi \| p)$
 - 4: Initialize dataset $D = \emptyset$
 - 5: **while** *True* **do**
 - 6: Sample initial state $s_0 \sim p_0$
 - 7: **while** s_h is not terminal **do**
 - 8: Sample weights $\theta \sim q_\xi(\theta)$
 - 9: Take action $a_h = \arg \max_a Q_\theta(s_h, a)$
 - 10: $s_{h+1} \sim \mathcal{P}_t(\cdot | s_h, a_h)$, $r_{h+1} = \mathcal{R}_i(s_h, a_h)$
 - 11: $D \leftarrow D \cup \langle s_h, a_h, r_{h+1}, s_{h+1} \rangle$
 - 12: Estimate $\nabla_\xi \mathcal{L}(\xi)$ using $D' \subseteq D$
 - 13: Update ξ with $\nabla_\xi \mathcal{L}(\xi)$ using any optimizer
 - 14: **end while**
 - 15: **end while**
-

Therefore, the idea behind the variational transfer of value functions (Algorithm 1) is to alternate a sampling from the posterior on the optimal value function with the optimization of the posterior via $\nabla_\xi \mathcal{L}(\xi)$, assuming to have already solved a finite number of source tasks $\mathcal{M}_1 \dots \mathcal{M}_n$, which, in turn, implies having the set of their approximate solutions $\Theta_s = \{\theta_1, \dots, \theta_n\}$. The weight resampling can be interpreted as a guess on the task that we need to solve based on the current belief. After sampling, the algorithm acts on the RL problem as if such guess were correct and then will adjust the belief based on the new experience through the optimization

of the variational parameters ξ . Notice that, as long as $\nabla_\xi \mathcal{L}(\xi)$ can be efficiently computed, any approximator for the Q -functions and any prior/posterior distributions can be used. To this end, since the max operator in the temporal difference error of Equation (2) is not differentiable, the *mellow-max* is used instead, which is differentiable and was proven to converge to the same fixed point of the optimal Bellman operator in [37]. From now on, we will denote the mellow Bellman error with \tilde{B}_θ .

3 Time-Variant Kernel Density Estimation for Variational Transfer

In the context of this work, we will model the evolution of time over a discrete grid of asymptotically dense time instants. Let $\{\theta_{ij}\}_{j=1}^{M_i}$ be a set of independent solutions to the i^{th} task, observed at time $t_i = \frac{i}{n}$, $1 \leq i \leq n$, with $\theta_{ij} \in \mathbb{R}^p$ and $\theta_{ij} \sim P(\cdot, t_i)$. Notice that, at time t_i , we allow to tackle M_i times the task coming from the distribution $P(\cdot, t_i)$, for the sake of generality. Furthermore, let M_i be a discrete random variable for each i . Finally, let us introduce a Time-Variant Kernel Density Estimator of this form:

$$\hat{p}(\theta, t) = \frac{1}{a_0(-\rho) \bar{N} \lambda |H|^{\frac{1}{2}}} \sum_{i=1}^n K_T \left(\frac{t - t_i}{\lambda} \right) \sum_{j=1}^{M_i} K_S(H^{-\frac{1}{2}}(\theta - \theta_{ij})), \quad (3)$$

which is based on [11] and will be used as a prior in order to model a time-variant distribution on the solved tasks. The factor $a_0(-\rho) = \int_{-\rho}^1 K_T(t) dt$ is used to perform the boundary correction, recovering consistency at the boundaries [13], therefore also in $t = 1$. K_T is the temporal kernel, whereas K_S is the multivariate non-negative spatial kernel. Furthermore, H is the spatial kernel bandwidth matrix, $\lambda \in [0, 1]$ is the temporal kernel bandwidth, and $\bar{N} = \sum_{i=1}^n M_i$.

Now under the following assumptions (also stated in [11]):

Assumption 3.1 (Task independence). For $1 \leq i \neq i' \leq n, 1 \leq j \leq M_i$, and $1 \leq j' \leq M_{i'}$, θ_{ij} and $\theta_{i'j'}$ are independent;

Assumption 3.2 (Differentiable density function). $p(\theta, t) : \mathbb{R}^p \times (0, 1] \rightarrow \mathbb{R}$ is twice differentiable for every t, θ ;

Assumption 3.3 (Bounded derivatives). $p(\theta, t) : \mathbb{R}^p \times (0, 1] \rightarrow \mathbb{R}$ has two bounded derivatives;

Assumption 3.4 (On the spatial kernel). Let $\alpha = (\alpha_1, \dots, \alpha_p)$ be a multi-index, with $\alpha_i \geq 0$ for $i = 1, \dots, p$, $\theta^\alpha = \prod_{i=1}^p \theta_i^{\alpha_i}$ for each $\theta \in \mathbb{R}^p$, and N_0 is an index set where all p components of each member are either 0 or even integers.

$$\int_{\mathbb{R}^p} K_S(\theta) d\theta = 1, \lim_{\|\theta\| \rightarrow \infty} \|\theta\|^p K_S(\theta) = 0, \int_{\mathbb{R}^p} \theta^\alpha K_S(\theta) d\theta = \mu_\alpha \leq \infty, \alpha \in N_0, \\ \int_{\mathbb{R}^p} \theta^\alpha K_S(\theta) d\theta = 0, \alpha \notin N_0;$$

Assumption 3.5 (On the temporal kernel).

$$\int_{-c}^c K_T(t) dt = 1, \int_{-c}^c t K_T(t) dt = 0, \int_{-c}^c t^2 K_T(t) dt = \sigma_T \leq \infty;$$

we can write

Theorem 3.6 (Uniform consistency of the density estimator). Assume 3.1 - 3.5. Moreover, assume that K_S is spherically symmetric, with a bounded, Hölder-continuous derivative, that K_T is a compactly supported kernel on a subset of \mathbb{R} , that all the M_i s are independent and identically distributed random variables with mean $m > 0$ and all moments finite, independent of the θ_{ij} s. Take H and λ such that $|H|^{\frac{1}{2}}(n) \rightarrow 0$, $\lambda(n) \rightarrow 0$ and $n^{1-\epsilon}|H|^{\frac{1}{2}}\lambda \rightarrow \infty$ for some $\epsilon > 0$ as $n \rightarrow \infty$, then

$$\hat{p}(\theta, t) = p(\theta, t) + O[(\bar{N}|H|^{\frac{1}{2}}\lambda)^{-\frac{1}{2}}(\log n)^{\frac{1}{2}} + \text{tr}(H) + \lambda]$$

uniformly in $(\theta, t) \in \mathcal{K} \times \mathcal{I}$, with probability 1, where \mathcal{K} is a compact subset of \mathbb{R}^p and \mathcal{I} is a compact subset of $(0, 1]$.

A proof of the above theorem is shown in Appendix A and leverages the same approach as in [11] being a weaker version, in terms of convergence rate, of their Theorem 1. This weakening was necessary to obtain an upper bound in closed-form expression of the KL-divergence between the prior and the posterior in Equation (2). Indeed, if we choose $q_\xi(\theta) = \frac{1}{K} \sum_{k=1}^K \mathcal{N}(\theta | \mu_k, \Sigma_k)$, with variational parameter $\xi = (\mu_1, \dots, \mu_K, \Sigma_1, \dots, \Sigma_K)$, and we choose K_S as a Gaussian kernel, then for a fixed time instant t our prior is a mixture of Gaussians with non-uniform weights. Therefore, through the upper bound on the KL-divergence shown in Appendix B, we have that the ELBO upper bounds the KL-divergence between the approximate and the exact posterior. Since the covariance matrices of the posterior must be positive definite, we will learn the factor L of their Cholesky decomposition as in [37].

Before going on with the finite sample analysis of the following section, we would like to discuss the previous assumptions and their potential limiting effects on applications. For what concerns Assumptions 3.4 and 3.5 they do not pose any limit, since, as we know from kernel density estimation theory, the kernel type is not so relevant for a good estimate of the density. Assumptions 3.2 and 3.3, instead, are necessary in order to have some degree of regularity allowing learning of the time-variant distribution (without those assumption the kernel density estimator would not be consistent). The range of time-variant distributions where our approach will be theoretically effective is reduced due to Assumptions 3.2 and 3.3, but remains still relevant from an application point of view.

4 Finite Sample Analysis

In order to provide a finite sample analysis of Algorithm 1 based on the prior of Section 3, we will extend Theorem 2 of [37] in our context, enabling also a theoretical comparison between the two respective versions of Algorithm 1. Therefore, considering the family of linearly parametrized value functions, $Q_\theta(s, a) = \theta^T \phi(s, a)$, having bounded weights $\|\theta\|_2 \leq \theta_{max}$ and uniformly bounded features $\|\phi(s, a)\|_2 \leq \phi_{max}$, and assuming that only finite data are available, we can bound the expected mellow Bellman error under the variational distribution minimizing Equation (2) for any fixed target task \mathcal{M}_t through the following theorem.

Theorem 4.1 (Bound on the expected mellow Bellman error). *Let $\hat{\xi}$ be the variational parameter minimizing Equation (2) on a dataset D of N i.i.d. samples distributed according to \mathcal{M}_t and ν . Moreover, let $\theta^* = \arg \inf_{\theta} \|\tilde{B}_{\theta}\|_{\nu}^2$ and define $v(\theta^*) = \mathbb{E}_{\mathcal{N}(\theta^*, \frac{1}{N}I)}[v(\theta)]$, with $v(\theta) = \mathbb{E}_{\nu}[\text{Var}_{\mathcal{P}_t}[\tilde{b}(\theta)]]$, where $\tilde{b}(\theta) = r + \gamma \text{mellow-max}_{a'} Q_{\theta}(s', a') - Q_{\theta}(s, a)$. Then, there exist constants c_1, c_2, c_3 such that with probability at least $1 - \delta$ over the choice of D :*

$$\mathbb{E}_{q_{\xi}} \left[\|\tilde{B}_{\theta}\|_{\nu}^2 \right] \leq 2 \|\tilde{B}_{\theta^*}\|_{\nu}^2 + v(\theta^*) + c_1 \sqrt{\frac{\log \frac{2}{\delta}}{N}} + \frac{c_2 + \psi p \log N + \psi \varphi(\Theta_s)}{N} + \frac{c_3}{N^2},$$

where

$$\varphi(\Theta_s) = \frac{1}{\sigma^2} \sum_{j: \theta_j \in \Theta_s} \frac{c_j^{\hat{p}} e^{-\beta \|\theta^* - \theta_j\|}}{\sum_{j': \theta_{j'} \in \Theta_s} c_{j'}^{\hat{p}} e^{-\beta \|\theta^* - \theta_{j'}\|}} \|\theta^* - \theta_j\|, \quad (4)$$

assuming the matrix H of Equation (3) to be an isotropic covariance matrix with variance σ^2 , $\beta = \frac{1}{2\sigma^2}$ and $c_j^{\hat{p}}$ the weight assigned to the j^{th} prior component. Furthermore, we are assuming $M_i = 1$ for each i in our estimator.

The above theorem shows the difference between the plain mixture version of Algorithm 1 [37] and our solution. Indeed, looking at $\varphi(\Theta_s)$, we are able to shed some light on the different theoretical properties of the two versions. More specifically, in the plain mixture version, factor $c_j^{\hat{p}}$ does not appear, which implies uniform importance of the source solutions Θ_s w.r.t. the target task. On the other hand, in our version of the algorithm, we are able to give different importance to each source solution through $c_j^{\hat{p}}$. In our time-variant scenario, this importance will be greater on more recent solutions than older ones, potentially allowing a reduction of the term $\varphi(\Theta_s)$ in contrast to the time-invariant version. A proof for the above theorem is provided in Appendix C.

5 Related Works

Our work is built upon [37], but differs from it because we leverage a time-variant structure underlying the task generating process, which is not taken into account in [37]. A theoretical comparison between the two solutions is available in Section 4 through Theorem 4.1, whereas the experimental comparison is in Section 6. Furthermore, our work relates both to [40], which deals with finite MDPs, and to [19], which leverages the commonalities in the value function structure, but, in contrast to our work, they do not account for a time-variant distribution. The work done in [6, 15, 28] leverage latent embeddings in order to model variations between tasks, which eventually are solved through a model-based RL algorithm, while we propose a model-free approach.

Another related work is [10], in which the authors develop a theoretical low-regret algorithm accounting for potential underlying dynamics. However, they use the online learning framework, whereas we are working in a transfer learning setting. Furthermore, in [8], videos are used to learn a prior (mainly to model the physical dynamics) which is incorporated into a model-based RL algorithm. In [41], a single-episode policy-transfer methodology was developed leveraging variational inference, but for contexts in which the differences in dynamics can be identified in the early steps of an episode. In the context of supervised learning, our work relates also to [25], which proposes a transfer learning mechanism in the context of a possibly non-stationary environment through a weighting approach, and [24, 7], which, instead, do transfer in non-stationary environments through ensembles. Finally, in [14] the authors are able to consider optimal initializations varying through time, but they develop this approach for a meta-learning framework, while our work considers a transfer learning setting.

6 Experiments

In this section, we compare our time-variant solution for transfer learning with the associated non-time-variant solution of [37] in three different domains with three different temporal dynamics. A detailed description of the used parameters together with the analytical expression of the employed dynamics are provided in Appendix D.

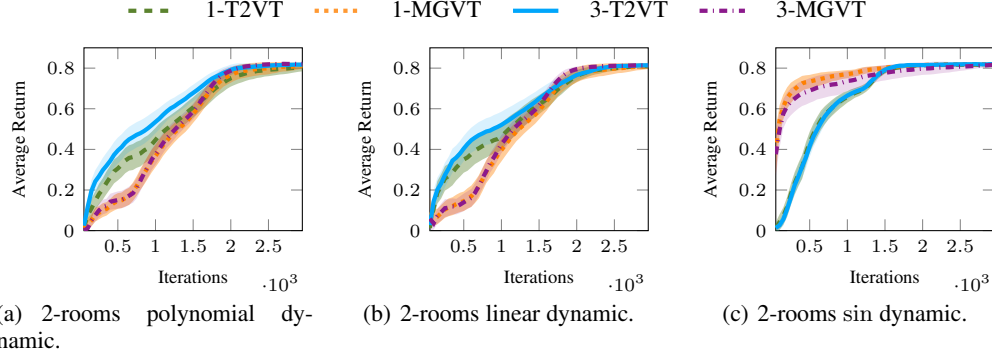


Figure 1: Average return achieved by the algorithms with 95% confidence intervals computed using 50 independent runs.

6.1 Temporal Dynamics

The distribution over the tasks is usually a given distribution over one or more parameters defining the task itself. Therefore, in order to obtain time-variance in such distribution, we will change its mean over time according to a certain dynamic. These dynamics are linear, polynomial, and sinusoidal. In the context of these experiments, we will use a time-variant Gaussian distribution, clipping its realizations within the domain of the parameters defining the task (for further details see Appendix D).

6.2 Two-Rooms Environment

In this setting, we have an agent navigating two rooms separated by a wall. The agent starts from the bottom-left corner and must reach the opposite one. The only way to reach this goal is to pass through the door whose position is unknown to the agent. The actions available to the agent are *up*, *down*, *left*, and *right*, which allow the agent to move in the respective directions by one position, unless he/she hits a wall (in this last case the position remains unchanged). Furthermore, the final position of the agent after a movement action is altered by a Gaussian noise $\mathcal{N}(0, 0.2)$. The state space is modeled through a 10×10 continuous grid. Finally, the reward function is 0 everywhere except in the goal state, where it is 1. The discount factor $\gamma = 0.99$. For this setting, we used linearly parametrized Q -functions with 121 evenly-spaced radial basis features.

We considered source tasks taken at ten different time instants to learn the target, corresponding to the eleventh instant of time. We sampled five tasks from the time-variant distribution for each $i = 1, \dots, 11$. The parameter that defines the task is the door location, hence the time-variant distribution is over that parameter, as we mentioned above. We solve all the source tasks by directly minimizing the TD error, then we exploit the learned solutions to perform the transfer over the target. We compare our time-variant variational transfer algorithm leveraging a c -components posterior (c -T2VT) with the mixture of Gaussian variational transfer using still c -components (c -MGVT) [37]. More specifically, our time-variant prior will consider the source task solutions as equally spaced samples in the time interval $[0, 1]$, moreover, in order to perform transfer to the eleventh task, we will use the distribution provided by our estimator for $t = 1$. Finally, the temporal kernel will be Epanechnikov in the context of all the experiments.

The average return over the last 50 learning episodes as a function of the number of training iterations is shown in Figure 1, for the time dynamics mentioned in Section 6.1. Each learning curve is computed using 50 independent runs, each of which resamples both the source and target tasks, with 95% confidence intervals. For polynomial and linear dynamics, we can see an advantage of our technique in the early learning iterations. The sinusoidal dynamic is designed to disadvantage our technique w.r.t. c -MGVT, indeed, it makes the target task appear twice in the sources. This fact inevitably favors c -MGVT, which will give a higher weight to those source tasks being sampled from the same distribution of the target. Observe that c -MGVT gives uniform weights to all the source tasks, hence increasing the replicas importance within the sources, whereas c -T2VT gives increasing weights the more recent the source solution.

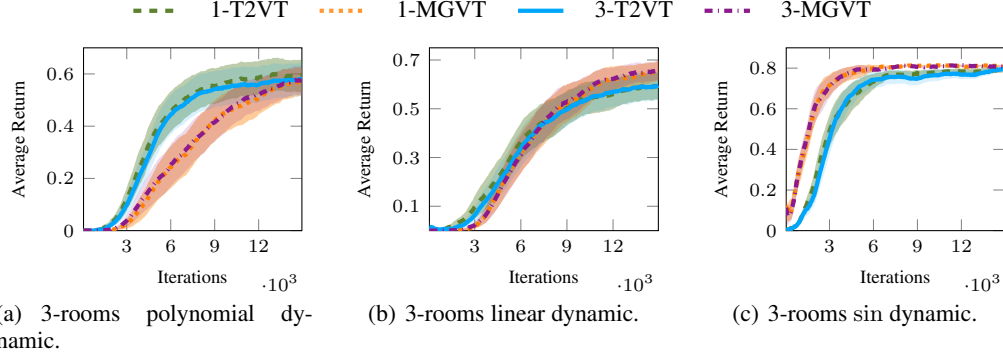


Figure 2: Average return achieved by the algorithms with 95% confidence intervals computed using 50 independent runs.

6.3 Three-Rooms Environment

This scenario is an extension of the previous one, hence the environmental settings remain the same, the agent has just an additional wall to traverse in order to reach his/her goal. Of course, the position of the door for this additional wall is still unknown to the agent. To increase the complexity of the dynamics, we let the two doors move in opposite directions starting at the two far ends of the room, each door with the same dynamic. In Figure 2, we compare c -T2VT with c -MGVT using still 95% confidence intervals. As for the polynomial dynamics, we observe a better performance of c -T2VT w.r.t. c -MGVT, whereas, for the sinusoidal dynamics, we have essentially the same behavior as in the two rooms environment. Finally, in the linear dynamics, we observe that the difference in performance between the two algorithms is not statistically significant.

6.4 Mountain Car

In this section, we consider a classic control environment known as Mountain Car [32]. In Mountain Car the agent is an underpowered car whose goal is to escape from a valley. Due to the limitation to its engine, the car has to alternately drive up along the two slopes of the valley in order to gain sufficient momentum to overcome gravity. In Figure 3, we have a comparison between c -T2VT and c -MGVT on the three proposed dynamics. We observe a statistically significant improvement in the polynomial dynamics across the whole learning process for c -T2VT, which also extends to the sinusoidal dynamic case. We would like to highlight the differences between the sinusoidal dynamic in Mountain Car w.r.t. the previous two environments. Here our algorithm is able to perform better due to a bias-variance trade-off in its favor. More specifically, the value functions vary more rapidly in Mountain Car than in the room environments w.r.t. a change in the task-defining parameters. Therefore, our prior estimator has less variance, since it considers only the latest sources, at the cost of a bias increase, because it discards the first task, which has the same parametrization as the target (due to the periodicity of the sin function). c -MGVT considers all the source tasks with the same uniform weight, hence it is able to consider the tasks that have an equivalent parametrization to the target, but are farther behind in the history of the sources. This fact decreases the bias at the cost of accepting a greater variance in the prior estimation. In Mountain Car the trade-off proposed by our algorithm is more advantageous than the one proposed by c -MGVT due to the more rapidly changing behavior of the value functions. As for the linear dynamics, we do not observe a statistically significant difference in performance between the two algorithms.

6.5 Choosing λ through Maximum-Likelihood

Up to now, we have kept λ and H at given constant values in order to allow a more faithful comparison between c -T2VT and c -MGVT (the matrix H was the same in the two algorithms whereas λ was set to 0.3333 leveraging the intuition that the more recent tasks were more important than the older ones). Of course, from the theory of Kernel Density Estimation, we know that appropriately setting these parameters is crucial to get a good estimate of the density. Therefore, an automatic data-driven approach would be desirable. In the context of this work, we propose a maximum likelihood scheme

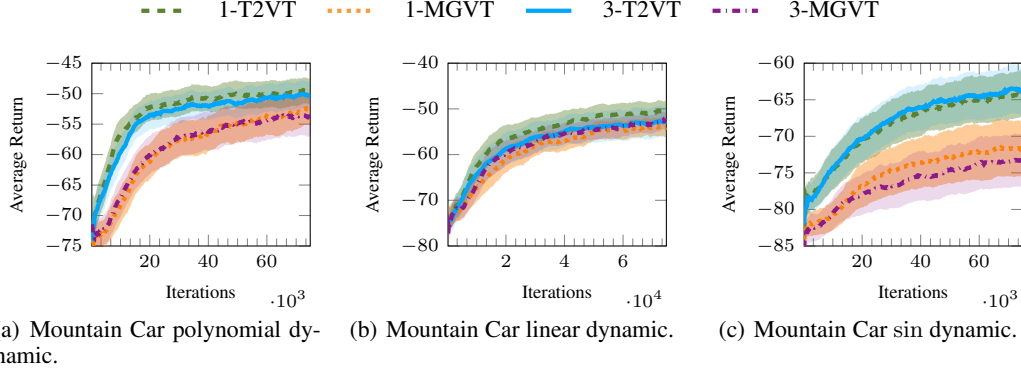


Figure 3: Average return achieved by the algorithms with 95% confidence intervals computed using 50 independent runs.

(assuming $M_i = 1 \forall i$):

$$\begin{aligned}
 \arg \max_{\lambda} L_{\lambda} &= \prod_{h=1}^n \frac{\hat{p}_{-h}(\theta_h, t_h)}{\hat{p}_{-h}(t_h)}, \text{ where} \\
 \hat{p}_{-h}(\theta_h, t_h) &= \frac{1}{a_0(-\rho)(\bar{N}-1)\lambda|H|^{\frac{1}{2}}} \sum_{i \neq h} K_T\left(\frac{t_h - t_i}{\lambda}\right) K_S(H^{-\frac{1}{2}}(\theta_h - \theta_i)) \\
 \hat{p}_{-h}(t_h) &= \int \hat{p}_{-h}(\theta_h, t_h) d\theta_h = \frac{1}{a_0(-\rho)(\bar{N}-1)\lambda} \sum_{i \neq h} K_T\left(\frac{t_h - t_i}{\lambda}\right).
 \end{aligned} \tag{5}$$

In Appendix D.3, we report the performance achievable with this approach together with a sensitivity analysis w.r.t. the parameter λ . Furthermore, still in Appendix D.3, we include some implementation details related to the optimization of the likelihood function in Equation (5). Note that, in accordance with what has been done in [37], the spatial bandwidth is set to $10^{-5}I$ which would prevent us from successfully optimizing Equation (5) due to numerical issues, hence we set it to I in order to select the best lambda.

7 Discussion and Conclusions

In this paper, we presented a time-variant approach for transferring value functions through a variational scheme. In order to deal with a time-variant distribution of the tasks, we have devised a suitable estimator for the prior to be used in the variational scheme providing its uniform consistency over a compact subset of $\mathbb{R}^p \times (0, 1]$. We have, then, provided a finite sample analysis on the performance of the variational transfer algorithm based on our estimator, enabling a theoretical comparison with the time-invariant version of [37]. Finally, we have experimentally proved our algorithm abilities to deal with time-variant distributions.

Notice that discriminating the source tasks according to time is an additional step that brings transfer learning approaches and learning in non-stationary environments a bit closer together [23]. It is also important to highlight the fact that, instead of considering time, we could switch to any other variable (e.g., the parameter defining the task itself, which, in the context of Mountain Car, is the base speed of the agent) as long as it is available together with each source solution and we can properly remap it into $(0, 1]$. This could allow us to leverage completely different structures in order to perform transfer to the target task. Moreover, in order to further improve the capabilities of the algorithm to deal with time-variant distributions, it would be relevant to leverage Gaussian Processes with a non-stationary covariance function as future work [30]. Finally, we would also like to highlight the possibility of using this time-variant transfer paradigm also in lifelong learning scenarios [5] as a potential future direction.

Broader Impact

Leveraging the time-variant structure in transfer learning tasks strengthens the bond of transfer learning itself with different other fields such as learning in non-stationary environments and life-long learning. This could potentially allow the exploitation of transfer learning into the previously mentioned fields, giving life to new advancements. Furthermore, being able to take into account the previously mentioned structure gives access to one more tool to deal with real-world applications, which are often time-variant, with a potential reduction for the time-to-market of RL based systems. This tool could be leveraged in order to make an RL system more able to adapt through time. Therefore, it could give a greater societal trust toward this system or, on the other hand, could potentially increase mistrust due to a higher decision-making power given to the system itself. In both cases, more awareness on the part of the general public towards artificial intelligence is needed in order to both avoid overconfidence and blind mistrust of these systems.

Acknowledgments and Disclosure of Funding

Use unnumbered first level headings for the acknowledgments. All acknowledgments go at the end of the paper before the list of references. Moreover, you are required to declare funding (financial activities supporting the submitted work) and competing interests (related financial activities outside the submitted work). More information about this disclosure can be found at: <https://neurips.cc/Conferences/2020/PaperInformation/FundingDisclosure>.

Do **not** include this section in the anonymized submission, only in the final paper. You can use the ack environment provided in the style file to automatically hide this section in the anonymized submission.

References

- [1] Maruan Al-Shedivat, Trapit Bansal, Yuri Burda, Ilya Sutskever, Igor Mordatch, and Pieter Abbeel. Continuous adaptation via meta-learning in nonstationary and competitive environments. *arXiv preprint arXiv:1710.03641*, 2017.
- [2] André Barreto, Will Dabney, Rémi Munos, Jonathan J Hunt, Tom Schaul, Hado P van Hasselt, and David Silver. Successor features for transfer in reinforcement learning. In *Advances in neural information processing systems*, pages 4055–4065, 2017.
- [3] David M Blei, Alp Kucukelbir, and Jon D McAuliffe. Variational inference: A review for statisticians. *Journal of the American statistical Association*, 112(518):859–877, 2017.
- [4] Olivier Catoni. Pac-bayesian supervised classification: the thermodynamics of statistical learning. *arXiv preprint arXiv:0712.0248*, 2007.
- [5] Zhiyuan Chen and Bing Liu. Lifelong machine learning. *Synthesis Lectures on Artificial Intelligence and Machine Learning*, 12(3):1–207, 2018.
- [6] Finale Doshi-Velez and George Konidaris. Hidden parameter markov decision processes: A semiparametric regression approach for discovering latent task parametrizations. In *IJCAI: proceedings of the conference*, volume 2016, page 1432. NIH Public Access, 2016.
- [7] Honghui Du, Leandro L Minku, and Huiyu Zhou. Multi-source transfer learning for non-stationary environments. In *2019 International Joint Conference on Neural Networks (IJCNN)*, pages 1–8. IEEE, 2019.
- [8] Yilun Du and Karthic Narasimhan. Task-agnostic dynamics priors for deep reinforcement learning. In *International Conference on Machine Learning*, pages 1696–1705, 2019.
- [9] Fernando Fernández and Manuela Veloso. Probabilistic policy reuse in a reinforcement learning agent. In *Proceedings of the fifth international joint conference on Autonomous agents and multiagent systems*, pages 720–727, 2006.
- [10] Eric C Hall and Rebecca M Willett. Online convex optimization in dynamic environments. *IEEE Journal of Selected Topics in Signal Processing*, 9(4):647–662, 2015.
- [11] Peter Hall, Hans-Georg Müller, and Ping-Shi Wu. Real-time density and mode estimation with application to time-dynamic mode tracking. *Journal of Computational and Graphical Statistics*, 15(1):82–100, 2006.

- [12] John R Hershey and Peder A Olsen. Approximating the kullback leibler divergence between gaussian mixture models. In *2007 IEEE International Conference on Acoustics, Speech and Signal Processing-ICASSP'07*, volume 4, pages IV–317. IEEE, 2007.
- [13] M Chris Jones. Simple boundary correction for kernel density estimation. *Statistics and computing*, 3(3):135–146, 1993.
- [14] Mikhail Khodak, Maria-Florina F Balcan, and Ameet S Talwalkar. Adaptive gradient-based meta-learning methods. In *Advances in Neural Information Processing Systems*, pages 5915–5926, 2019.
- [15] Taylor W Killian, Samuel Daulton, George Konidaris, and Finale Doshi-Velez. Robust and efficient transfer learning with hidden parameter markov decision processes. In *Advances in neural information processing systems*, pages 6250–6261, 2017.
- [16] Diederik P Kingma and Jimmy Ba. Adam: A method for stochastic optimization. *arXiv preprint arXiv:1412.6980*, 2014.
- [17] George Konidaris and Andrew G Barto. Building portable options: Skill transfer in reinforcement learning. In *IJCAI*, volume 7, pages 895–900, 2007.
- [18] Alessandro Lazaric. Transfer in reinforcement learning: a framework and a survey. In *Reinforcement Learning*, pages 143–173. Springer, 2012.
- [19] Alessandro Lazaric and Mohammad Ghavamzadeh. Bayesian multi-task reinforcement learning. In *Proceedings of the 27th International Conference on International Conference on Machine Learning*, pages 599–606, 2010.
- [20] Alessandro Lazaric, Marcello Restelli, and Andrea Bonarini. Transfer of samples in batch reinforcement learning. In *Proceedings of the 25th international conference on Machine learning*, pages 544–551, 2008.
- [21] Lucas Lehnert and Michael L Littman. Transfer with model features in reinforcement learning. *arXiv preprint arXiv:1807.01736*, 2018.
- [22] Odalric-Ambrym Maillard, Rémi Munos, Alessandro Lazaric, and Mohammad Ghavamzadeh. Finite-sample analysis of bellman residual minimization. In *Proceedings of 2nd Asian Conference on Machine Learning*, pages 299–314, 2010.
- [23] Leandro L Minku. Transfer learning in non-stationary environments. In *Learning from Data Streams in Evolving Environments*, pages 13–37. Springer, 2019.
- [24] Leandro L Minku and Xin Yao. Ddd: A new ensemble approach for dealing with concept drift. *IEEE transactions on knowledge and data engineering*, 24(4):619–633, 2011.
- [25] Leandro L Minku and Xin Yao. How to make best use of cross-company data in software effort estimation? In *Proceedings of the 36th International Conference on Software Engineering*, pages 446–456, 2014.
- [26] Anusha Nagabandi, Ignasi Clavera, Simin Liu, Ronald S Fearing, Pieter Abbeel, Sergey Levine, and Chelsea Finn. Learning to adapt in dynamic, real-world environments through meta-reinforcement learning. *arXiv preprint arXiv:1803.11347*, 2018.
- [27] OpenAI, Christopher Berner, Greg Brockman, Brooke Chan, Vicki Cheung, Przemysław Dębiak, Christy Dennison, David Farhi, Quirin Fischer, Shariq Hashme, Chris Hesse, Rafal Józefowicz, Scott Gray, Catherine Olsson, Jakub Pachocki, Michael Petrov, Henrique Pondé de Oliveira Pinto, Jonathan Raiman, Tim Salimans, Jeremy Schlatter, Jonas Schneider, Szymon Sidor, Ilya Sutskever, Jie Tang, Filip Wolski, and Susan Zhang. Dota 2 with large scale deep reinforcement learning. 2019.
- [28] Christian F Perez, Felipe Petroski Such, and Theofanis Karaletsos. Generalized hidden parameter mdps transferable model-based rl in a handful of trials. *arXiv preprint arXiv:2002.03072*, 2020.
- [29] Martin L Puterman. *Markov decision processes: discrete stochastic dynamic programming*. John Wiley & Sons, 2014.
- [30] Sami Remes, Markus Heinonen, and Samuel Kaski. Non-stationary spectral kernels. In *Advances in Neural Information Processing Systems*, pages 4642–4651, 2017.

- [31] David Silver, Thomas Hubert, Julian Schrittwieser, Ioannis Antonoglou, Matthew Lai, Arthur Guez, Marc Lanctot, Laurent Sifre, Dhharshan Kumaran, Thore Graepel, et al. A general reinforcement learning algorithm that masters chess, shogi, and go through self-play. *Science*, 362(6419):1140–1144, 2018.
- [32] Richard S Sutton and Andrew G Barto. Reinforcement learning: An introduction. 2011.
- [33] Matthew E Taylor, Nicholas K Jong, and Peter Stone. Transferring instances for model-based reinforcement learning. In *Joint European conference on machine learning and knowledge discovery in databases*, pages 488–505. Springer, 2008.
- [34] Matthew E. Taylor and Peter Stone. Transfer learning for reinforcement learning domains: A survey. *Journal of Machine Learning Research*, 10(56):1633–1685, 2009.
- [35] Matthew E Taylor, Peter Stone, and Yaxin Liu. Transfer learning via inter-task mappings for temporal difference learning. *Journal of Machine Learning Research*, 8(Sep):2125–2167, 2007.
- [36] Andrea Tirinzoni, Mattia Salvini, and Marcello Restelli. Transfer of samples in policy search via multiple importance sampling. In *International Conference on Machine Learning*, pages 6264–6274, 2019.
- [37] Andrea Tirinzoni, Rafael Rodriguez Sanchez, and Marcello Restelli. Transfer of value functions via variational methods. In *Advances in Neural Information Processing Systems*, pages 6179–6189, 2018.
- [38] Andrea Tirinzoni, Andrea Sessa, Matteo Pirota, and Marcello Restelli. Importance weighted transfer of samples in reinforcement learning. *arXiv preprint arXiv:1805.10886*, 2018.
- [39] Oriol Vinyals, Igor Babuschkin, Wojciech M Czarnecki, Michaël Mathieu, Andrew Dudzik, Junyoung Chung, David H Choi, Richard Powell, Timo Ewalds, Petko Georgiev, et al. Grandmaster level in starcraft ii using multi-agent reinforcement learning. *Nature*, 575(7782):350–354, 2019.
- [40] Aaron Wilson, Alan Fern, Soumya Ray, and Prasad Tadepalli. Multi-task reinforcement learning: a hierarchical bayesian approach. In *Proceedings of the 24th international conference on Machine learning*, pages 1015–1022, 2007.
- [41] Jiachen Yang, Brenden Petersen, Hongyuan Zha, and Daniel Faissol. Single episode policy transfer in reinforcement learning. In *International Conference on Learning Representations*, 2020.

A Proof of Theorem 3.6

Definition A.1. For a spatial kernel K_S : $\mu_l(K_S) = \int \theta^l K_S(\theta) d\theta$

Definition A.2. For a temporal kernel K_T : $a_l(-\rho) = \int_{-\rho}^1 t^l K_T(t) dt$

Lemma A.1 (Estimator consistency on the right boundary). *Let $t \in B_r = \{\tau : 1 - \lambda \leq \tau \leq 1\}$ then under assumptions of Theorem 3.6:*

$$\mathbb{E}[\hat{p}(\theta, t) | \mathcal{M}] = p(\theta, t) + O(\lambda) + O(\text{tr}(H)),$$

where \mathcal{M} represents all the discrete random variables M_i for $i = 1 \dots n$.

Proof.

$$\begin{aligned} \mathbb{E}[\hat{p}(\theta, t) | \mathcal{M}] &= \\ &= \frac{1}{N\lambda|H|^{\frac{1}{2}}a_0(-\rho)} \sum_{i=1}^n \int K_T\left(\frac{t-\tau}{\lambda}\right) \sum_{j=1}^{M_i} \int_{-\infty}^{+\infty} K_S\left(H^{-\frac{1}{2}}(\theta-x)\right) p(x, \tau) dx d\tau \end{aligned} \quad (6)$$

$$= \frac{1}{N\lambda|H|^{\frac{1}{2}}a_0(-\rho)} \sum_{i=1}^n \int K_T\left(\frac{t-\tau}{\lambda}\right) \sum_{j=1}^{M_i} \int_{-\infty}^{+\infty} -K_S(y)p(\theta - H^{\frac{1}{2}}y, \tau) dy d\tau \quad (7)$$

$$\begin{aligned} &= \frac{1}{N\lambda a_0(-\rho)} \sum_{i=1}^n \int K_T\left(\frac{t-\tau}{\lambda}\right) \sum_{j=1}^{M_i} \int_{-\infty}^{+\infty} K_S(y) \left(p(\theta, \tau) - (H^{\frac{1}{2}}y)^T \nabla^S p(\theta, \tau) + \right. \\ &\quad \left. \frac{1}{2} (H^{\frac{1}{2}}y)^T \mathcal{H}^S p(\theta, \tau) (H^{\frac{1}{2}}y) + o(\text{tr}(H)) \right) dy d\tau \end{aligned} \quad (8)$$

$$\begin{aligned} &= \frac{1}{N\lambda a_0(-\rho)} \sum_{i=1}^n \int K_T\left(\frac{t-\tau}{\lambda}\right) M_i \left(\int_{-\infty}^{+\infty} K_S(y) p(\theta, \tau) dy \right. \\ &\quad \left. - \int_{-\infty}^{+\infty} K_S(y) (H^{\frac{1}{2}}y)^T \nabla^S p(\theta, \tau) dy + \right. \\ &\quad \left. \int_{-\infty}^{+\infty} \frac{1}{2} K_S(y) (H^{\frac{1}{2}}y)^T \mathcal{H}^S p(\theta, \tau) (H^{\frac{1}{2}}y) dy + o(\text{tr}(H)) \right) d\tau \end{aligned} \quad (9)$$

$$\begin{aligned} &= \frac{1}{N\lambda a_0(-\rho)} \sum_{i=1}^n \int K_T\left(\frac{t-\tau}{\lambda}\right) M_i \left(p(\theta, \tau) + \right. \\ &\quad \left. \frac{1}{2} \mu_2(K_S) \text{tr}(H \mathcal{H}^S p(\theta, \tau)) + o(\text{tr}(H)) \right) d\tau \end{aligned} \quad (10)$$

$$= \frac{1}{\lambda a_0(-\rho)} \int_{\frac{t-1}{\lambda}}^{\frac{t}{\lambda}} K_T\left(\frac{t-\tau}{\lambda}\right) \left(p(\theta, \tau) + O(\text{tr}(H)) \right) d\tau \quad (11)$$

$$= \frac{1}{\lambda a_0(-\rho)} \left(\int_{-\rho}^1 K_T\left(\frac{t-\tau}{\lambda}\right) p(\theta, \tau) d\tau + O(\text{tr}(H)) \int_{-\rho}^1 K_T\left(\frac{t-\tau}{\lambda}\right) d\tau \right) \quad (12)$$

$$= \frac{\lambda}{\lambda a_0(-\rho)} \left(- \int_1^{-\rho} K_T(v) p(\theta, t - \lambda v) dv - O(\text{tr}(H)) \int_1^{-\rho} K_T(v) dv \right) \quad (13)$$

$$\begin{aligned} &= \frac{1}{a_0(-\rho)} \left(\int_{-\rho}^1 K_T(v) \left(p(\theta, t) - \lambda v p'(\theta, t) + \right. \right. \\ &\quad \left. \left. \frac{1}{2} \lambda^2 v^2 p''(\theta, t) + o(\lambda^2) \right) dv + O(\text{tr}(H)) \right) \end{aligned} \quad (14)$$

$$= p(\theta, t) - \lambda p'(\theta, t) \frac{a_1(-\rho)}{a_0(-\rho)} + O(\lambda^2) + O(\text{tr}(H)) \quad (15)$$

$$= p(\theta, t) + O(\lambda) + O(\text{tr}(H)), \quad (16)$$

where in (7) we performed a change of variable, $y = H^{-\frac{1}{2}}(\theta - x)$, in (8) we used the following Taylor expansion:

$$p(\theta - H^{\frac{1}{2}}y, \tau) = p(\theta, \tau) - (H^{\frac{1}{2}}y)^T \nabla^S p(\theta, \tau) + \frac{1}{2}(H^{\frac{1}{2}}y)^T \mathcal{H}^S p(\theta, \tau)(H^{\frac{1}{2}}y) + o(\text{tr}(H)),$$

in (9) we used Assumption 3.4, in (10) we used Definition A.1, in (11) we used $\frac{t-\tau}{\lambda} \in [\frac{t-1}{\lambda}, \frac{t}{\lambda}]$, in 12 we set $t = 1 - \rho\lambda$, which implies $\frac{t-\tau}{\lambda} \in [-\rho, \frac{1}{\lambda} - \rho]$, then we used the support of K_T (assumed to be $[-1, 1]$ without loss of generality) since $\lambda \rightarrow 0$. Finally, in 13 we used a change of variable, $\frac{t-\tau}{\lambda} = v$, and in 14 we used the following Taylor expansion:

$$p(\theta, t - \lambda v) = p(\theta, t) - \lambda v p'(\theta, t) + \frac{1}{2} \lambda^2 v^2 p''(\theta, v) + o(\lambda^2).$$

□

Notice that we reported the consistency proof only on the right boundary because is the one we use in the context of our algorithm. The above procedure can be easily adjusted to prove consistency of the estimator on the left boundary getting the same convergence rate. Moreover, analogously, we can obtain consistency away from the two boundaries with a convergence rate squared w.r.t. λ .

Definition A.3. For a spatial kernel K_S : $R(K_S) = \int K_S^2(\theta) d\theta$

Definition A.4. For a temporal kernel K_T : $b_{K_T}(-\rho) = \int_{-\rho}^1 K_T^2(t) dt$

Lemma A.2 (Variance of the estimator on the right boundary). *Let $t \in B_r = \{\tau : 1 - \lambda \leq \tau \leq 1\}$ then under assumptions of Theorem 3.6:*

$$\mathbb{V}ar[\hat{p}(\theta, t) | \mathcal{M}] \leq \frac{C_1}{\bar{N} |H|^{\frac{1}{2}} \lambda},$$

where \mathcal{M} represents all the discrete random variables M_i for $i = 1 \dots n$.

Proof.

$$\mathbb{V}ar[\hat{p}(\theta, t)|\mathcal{M}] = \frac{1}{Na_0^2(-\rho)} \mathbb{V}ar \left[\frac{1}{|H|^{\frac{1}{2}}\lambda} K_T \left(\frac{t-t_i}{\lambda} \right) K_S \left(H^{-\frac{1}{2}}(\theta - x_{ij}) \right) \right] \quad (17)$$

$$= \frac{1}{Na_0^2(-\rho)} \left(\mathbb{E} \left[\frac{1}{|H|\lambda^2} K_T^2 \left(\frac{t-t_i}{\lambda} \right) K_S^2 \left(H^{-\frac{1}{2}}(\theta - x_{ij}) \right) \right] - \mathbb{E}^2 \left[\frac{1}{|H|^{\frac{1}{2}}\lambda} K_T \left(\frac{t-t_i}{\lambda} \right) K_S \left(H^{-\frac{1}{2}}(\theta - x_{ij}) \right) \right] \right) \quad (18)$$

$$= \frac{1}{Na_0^2(-\rho)} \left(\int \frac{1}{|H|\lambda^2} K_T^2 \left(\frac{t-\tau}{\lambda} \right) \int_{+\infty}^{-\infty} -|H|^{\frac{1}{2}} K_S^2(y) p(\theta - H^{\frac{1}{2}}y, \tau) dy d\tau - \left(\int \frac{1}{|H|^{\frac{1}{2}}\lambda} K_T \left(\frac{t-\tau}{\lambda} \right) \int_{+\infty}^{-\infty} -|H|^{\frac{1}{2}} K_S(y) p(\theta - H^{\frac{1}{2}}y, \tau) dy d\tau \right)^2 \right) \quad (19)$$

$$= \frac{1}{Na_0^2(-\rho)} \left(\int \frac{1}{|H|^{\frac{1}{2}}\lambda^2} K_T^2 \left(\frac{t-\tau}{\lambda} \right) \int_{-\infty}^{+\infty} K_S^2(y) (p(\theta, \tau) + o(1)) dy d\tau - \left(\int \frac{1}{\lambda} K_T \left(\frac{t-\tau}{\lambda} \right) \int_{-\infty}^{+\infty} K_S(y) (p(\theta, \tau) + o(1)) dy d\tau \right)^2 \right) \quad (20)$$

$$= \frac{1}{Na_0^2(-\rho)} \left(\int \frac{1}{|H|^{\frac{1}{2}}\lambda^2} K_T^2 \left(\frac{t-\tau}{\lambda} \right) (p(\theta, \tau) + o(1)) R(K_S) d\tau - \left(\int \frac{1}{\lambda} K_T \left(\frac{t-\tau}{\lambda} \right) (p(\theta, \tau) + o(1)) d\tau \right)^2 \right) \quad (21)$$

$$= \frac{1}{Na_0^2(-\rho)} \left(\int_{-\rho}^1 \frac{1}{|H|^{\frac{1}{2}}\lambda^2} K_T^2 \left(\frac{t-\tau}{\lambda} \right) (p(\theta, \tau) + o(1)) R(K_S) d\tau - \left(\int_{-\rho}^1 \frac{1}{\lambda} K_T \left(\frac{t-\tau}{\lambda} \right) (p(\theta, \tau) + o(1)) d\tau \right)^2 \right) \quad (22)$$

$$= \frac{1}{Na_0^2(-\rho)} \left(\int_1^{-\rho} -\frac{1}{|H|^{\frac{1}{2}}\lambda} K_T^2(v) (p(\theta, t - \lambda v) + o(1)) R(K_S) dv - \left(\int_1^{-\rho} -K_T(v) (p(\theta, t - \lambda v) + o(1)) dv \right)^2 \right) \quad (23)$$

$$= \frac{1}{Na_0^2(-\rho)} \left(\int_{-\rho}^1 \frac{1}{|H|^{\frac{1}{2}}\lambda} K_T^2(v) (p(\theta, t) + o(1)) R(K_S) dv - \left(\int_{-\rho}^1 K_T(v) (p(\theta, t) + o(1)) dv \right)^2 \right) \quad (24)$$

$$= \frac{1}{Na_0^2(-\rho)} \left(\frac{p(\theta, t) + o(1)}{|H|^{\frac{1}{2}}\lambda} R(K_S) b_{K_T}(-\rho) - (a_0(-\rho)(p(\theta, t) + o(1)))^2 \right) \quad (25)$$

$$= \frac{p(\theta, t) R(K_S) b_{K_T}(-\rho)}{\bar{N}|H|^{\frac{1}{2}}\lambda a_0^2(-\rho)} + O \left(\frac{1}{\bar{N}|H|^{\frac{1}{2}}\lambda} \right) \quad (26)$$

$$= O \left(\frac{1}{\bar{N}|H|^{\frac{1}{2}}\lambda} \right) \rightarrow \exists C_1 : \mathbb{V}ar[\hat{p}(\theta, t)|\mathcal{M}] \leq \frac{C_1}{\bar{N}|H|^{\frac{1}{2}}\lambda}, \quad (27)$$

where in (19) we performed a change of variable, $y = H^{-\frac{1}{2}}(\theta - x)$, in (20) we used the following Taylor expansion:

$$p(\theta - H^{\frac{1}{2}}y, \tau) = p(\theta, \tau) + o(1),$$

in 21 we used Definition A.3, in 22 we considered the fact that $t \in B_r$ as we have done in 11 and 12 of the proof of A.1, in 23 we performed a change of variable, $\frac{t-\tau}{\lambda} = v$, in 24 we used the following Taylor expansion:

$$p(\theta, t - \lambda v) = p(\theta, t) + o(1),$$

whereas in 25 we have used Definition A.4. Finally, in 27 we have used the fact that $p(\theta, t)$ has bounded derivatives and is a pdf, therefore it has finite supremum. \square

Lemma A.3 (Bound on the absolute values). *Let $t \in B_r = \{\tau : 1 - \lambda \leq \tau \leq 1\}$ then under assumptions of Theorem 3.6: $\hat{p}(\theta, t) - \mathbb{E}[\hat{p}(\theta, t)|\mathcal{M}]$ is the sum of \bar{N} independent random variables, denoted as v_i , with zero mean and absolute values bounded by $\frac{C_2}{\bar{N}|H|^{\frac{1}{2}\lambda}}$. \mathcal{M} represents all the discrete random variables M_i for $i = 1 \dots n$.*

Proof.

$$|v_i| = \left| \frac{1}{\bar{N}\lambda|H|^{\frac{1}{2}\lambda}a_0(-\rho)} K_T\left(\frac{t-t_i}{\lambda}\right) K_S(H^{-\frac{1}{2}}(\theta - x_{ij})) - \frac{p(\theta, t) + O(\lambda) + O(\text{tr}(H))}{\bar{N}} \right| \quad (28)$$

$$\leq \left| \frac{M_T M_S}{\bar{N}\lambda|H|^{\frac{1}{2}\lambda}a_0(-\rho)} - \frac{p(\theta, t) + O(\lambda) + O(\text{tr}(H))}{\bar{N}} \right| \quad (29)$$

$$= O\left(\frac{1}{\bar{N}\lambda|H|^{\frac{1}{2}\lambda}}\right) \rightarrow \exists C_2 : |v_i| \leq \frac{C_2}{\bar{N}|H|^{\frac{1}{2}\lambda}}, \quad (30)$$

where in 28 we used lemma A.1 and in 29 we used the fact that K_T has a compact support on \mathbb{R} and K_S has a supremum. \square

Now the proof of Theorem 3.6 can follow.

Proof. Let $\xi = C\left(\frac{\log n}{\bar{N}|H|^{\frac{1}{2}\lambda}}\right)^{\frac{1}{2}}$ and $C_3 = \frac{1}{\max(C_1, \frac{C_2}{3})}$, using Bernstein's inequality we can write:

$$\mathbb{P}(|\hat{p}(\theta, t) - \mathbb{E}[\hat{p}(\theta, t)|\mathcal{M}]| > \xi|\mathcal{M}) \leq 2 \exp\left(-\frac{\frac{1}{2}\xi^2}{\frac{C_1}{\bar{N}|H|^{\frac{1}{2}\lambda}} + \frac{1}{3}\frac{C_2\xi}{\bar{N}|H|^{\frac{1}{2}\lambda}}}\right) \quad (31)$$

$$= 2 \exp\left(-\frac{\frac{1}{2}C^2 \log n}{C_1 + \frac{1}{3}C_2\xi}\right) \leq 2 \exp\left(-\frac{C_3 C^2 \log n}{1 + \xi}\right), \forall(\theta, t). \quad (32)$$

Therefore, if $C_4 > 0$ is given, and we choose $C^2 > \frac{3C_4}{C_3}$, then we can write:

$$\sup_{(\theta, t) \in \mathbb{R}^p \times \mathcal{I}} \mathbb{P}\left(|\hat{p}(\theta, t) - \mathbb{E}[\hat{p}(\theta, t)|\mathcal{M}]| > C\left(\frac{\log n}{\bar{N}|H|^{\frac{1}{2}\lambda}}\right)^{\frac{1}{2}}\right) \leq 2 \exp\left(-\frac{3C_4 \log n}{1 + \xi}\right) \quad (33)$$

$$= 2n^{-\frac{3C_4}{1+\xi}}. \quad (34)$$

Now restricting to finite subsets $\mathcal{K}_n \subset \mathcal{K} \subset \mathbb{R}^p$ and $\mathcal{I}_n \subset \mathcal{I}$ where $\mathcal{K}_n \times \mathcal{I}_n$ has at most $\lfloor n^{\frac{2C_4}{1+\xi}} \rfloor$ elements, we have:

$$\mathbb{P}\left(\sup_{(\theta, t) \in \mathcal{K}_n \times \mathcal{I}_n} |\hat{p}(\theta, t) - \mathbb{E}[\hat{p}(\theta, t)|\mathcal{M}]| > C\left(\frac{\log n}{\bar{N}|H|^{\frac{1}{2}\lambda}}\right)^{\frac{1}{2}}\right) \leq 2n^{-\frac{3C_4}{1+\xi}}. \quad (35)$$

From the Hölder-continuity of the estimator (since the two kernels have bounded first derivative):

$$\begin{aligned} & \sup_{(\theta, t) \in \mathcal{K} \times \mathcal{I}} \{|\hat{p}(\theta, t) - \mathbb{E}[\hat{p}(\theta, t)|\mathcal{M}]\} - \sup_{(\theta, t) \in \mathcal{K}_n \times \mathcal{I}_n} \{|\hat{p}(\theta, t) - \mathbb{E}[\hat{p}(\theta, t)|\mathcal{M}]\} = \\ & \left| \sup_{(\theta, t) \in \mathcal{K} \times \mathcal{I}} \{|\hat{p}(\theta, t) - \mathbb{E}[\hat{p}(\theta, t)|\mathcal{M}]\} - \sup_{(\theta, t) \in \mathcal{K}_n \times \mathcal{I}_n} \{|\hat{p}(\theta, t) - \mathbb{E}[\hat{p}(\theta, t)|\mathcal{M}]\} \right| \leq \\ & \left| \sup_{(\theta, t) \in \mathcal{K} \times \mathcal{I}} \{\hat{p}(\theta, t) - \mathbb{E}[\hat{p}(\theta, t)|\mathcal{M}]\} - \sup_{(\theta, t) \in \mathcal{K}_n \times \mathcal{I}_n} \{\hat{p}(\theta, t) - \mathbb{E}[\hat{p}(\theta, t)|\mathcal{M}]\} \right| \leq \\ & D\|v^* - v_n^*\|^\alpha, \end{aligned} \quad (36)$$

where

$$\begin{aligned} v^* &= \arg \sup_{(\theta, t) \in \mathcal{K} \times \mathcal{I}} \{\hat{p}(\theta, t) - \mathbb{E}[\hat{p}(\theta, t) | \mathcal{M}]\} \\ v_n^* &= \arg \sup_{(\theta, t) \in \mathcal{K}_n \times \mathcal{I}_n} \{\hat{p}(\theta, t) - \mathbb{E}[\hat{p}(\theta, t) | \mathcal{M}]\}, \end{aligned}$$

therefore:

$$\begin{aligned} \mathbb{P} \left(\sup_{(\theta, t) \in \mathcal{K} \times \mathcal{I}} |\hat{p}(\theta, t) - \mathbb{E}[\hat{p}(\theta, t) | \mathcal{M}]| > C \left(\frac{\log n}{\bar{N} |H|^{\frac{1}{2}} \lambda} \right)^{\frac{1}{2}} + D \|v^* - v_n^*\|^\alpha \right) \leq \\ \mathbb{P} \left(\sup_{(\theta, t) \in \mathcal{K}_n \times \mathcal{I}_n} |\hat{p}(\theta, t) - \mathbb{E}[\hat{p}(\theta, t) | \mathcal{M}]| > C \left(\frac{\log n}{\bar{N} |H|^{\frac{1}{2}} \lambda} \right)^{\frac{1}{2}} \right) \end{aligned} \quad (37)$$

now, for sufficiently large C_4 , $\|v^* - v_n^*\| \leq \frac{\sqrt{p+1}}{2} \sqrt[p+1]{\frac{(K_{max} - K_{min})^p (I_{max} - I_{min})}{\lfloor n^{\frac{2C_4}{1+\xi}} \rfloor}}$ and

$D \left(\frac{\sqrt{p+1}}{2} \sqrt[p+1]{\frac{(K_{max} - K_{min})^p (I_{max} - I_{min})}{\lfloor n^{\frac{2C_4}{1+\xi}} \rfloor}} \right)^\alpha$ is negligible w.r.t. ξ as n tends to infinity, where

K_{max} e K_{min} are the endpoints for each dimension of \mathcal{K} (we assume them to be the same in each dimension for the sake of simplicity). Analogously for I_{max} and I_{min} (notice that \mathcal{I} is monodimensional).

Therefore:

$$\begin{aligned} \mathbb{P} \left(\sup_{(\theta, t) \in \mathcal{K} \times \mathcal{I}} |\hat{p}(\theta, t) - \mathbb{E}[\hat{p}(\theta, t) | \mathcal{M}]| > C \left(\frac{\log n}{\bar{N} |H|^{\frac{1}{2}} \lambda} \right)^{\frac{1}{2}} + \right. \\ \left. D \left(\frac{p+1}{4} \right)^{\frac{\alpha}{2}} \left(\frac{(K_{max} - K_{min})^p (I_{max} - I_{min})}{\lfloor n^{\frac{2C_4}{1+\xi}} \rfloor} \right)^{\frac{\alpha}{p+1}} \right) \leq \\ \mathbb{P} \left(\sup_{(\theta, t) \in \mathcal{K}_n \times \mathcal{I}_n} |\hat{p}(\theta, t) - \mathbb{E}[\hat{p}(\theta, t) | \mathcal{M}]| > C \left(\frac{\log n}{\bar{N} |H|^{\frac{1}{2}} \lambda} \right)^{\frac{1}{2}} \right). \end{aligned} \quad (38)$$

From (35) and (38), we can write:

$$\begin{aligned} \mathbb{P} \left(\sup_{(\theta, t) \in \mathcal{K} \times \mathcal{I}} |\hat{p}(\theta, t) - \mathbb{E}[\hat{p}(\theta, t) | \mathcal{M}]| < C \left(\frac{\log n}{\bar{N} |H|^{\frac{1}{2}} \lambda} \right)^{\frac{1}{2}} + \right. \\ \left. D \left(\frac{p+1}{4} \right)^{\frac{\alpha}{2}} \left(\frac{(K_{max} - K_{min})^p (I_{max} - I_{min})}{\lfloor n^{\frac{2C_4}{1+\xi}} \rfloor} \right)^{\frac{\alpha}{p+1}} \right) \geq 1 - 2n^{-\frac{C_4}{1+\xi}} \end{aligned} \quad (39)$$

Therefore, as $n \rightarrow \infty$ with probability 1:

$$\begin{aligned} |\hat{p}(\theta, t) - p(\theta, t) - O(\lambda) - O(\text{tr}(|H|))| = O \left[C \left(\frac{\log n}{\bar{N} |H|^{\frac{1}{2}} \lambda} \right)^{\frac{1}{2}} + \right. \\ \left. D \left(\frac{p+1}{4} \right)^{\frac{\alpha}{2}} \left(\frac{(K_{max} - K_{min})^p (I_{max} - I_{min})}{\lfloor n^{\frac{2C_4}{1+\xi}} \rfloor} \right)^{\frac{\alpha}{p+1}} \right], \forall (\theta, t) \in \mathcal{K} \times \mathcal{I} \end{aligned} \quad (40)$$

Finally, we get:

$$\hat{p}(\theta, t) = p(\theta, t) + O \left[\left(\frac{\log n}{\bar{N} |H|^{\frac{1}{2}} \lambda} \right)^{\frac{1}{2}} + \lambda + \text{tr}(H) \right], \forall (\theta, t) \in \mathcal{K} \times \mathcal{I} \quad (41)$$

□

B Upper bound on the KL-Divergence between the prior and the posterior

In this section, we report the steps needed to get an upper bound on the KL-Divergence between the posterior q our prior \hat{p} . Let us define $S = \frac{1}{a_0(-\rho)N\lambda} \sum_{i=1}^n \sum_{j=1}^{M_i} K_T(\frac{t-t_i}{\lambda})$, hence:

$$D_{KL}(q||\hat{p}(\cdot, t)) = \int q(\theta) \log \frac{q(\theta)}{\hat{p}(\theta, t)} d\theta = \int q(\theta) \log \frac{q(\theta)}{\frac{1}{S} \hat{p}(\theta, t)} d\theta \quad (42)$$

$$= \int q(\theta) \log \frac{q(\theta)}{\frac{1}{S a_0(-\rho)N|H|^{\frac{1}{2}}\lambda} \sum_{i=1}^n K_T(\frac{t-t_i}{\lambda}) \sum_{j=1}^{M_i} K_S(H^{-\frac{1}{2}}(\theta - \theta_{ij}))} d\theta + \int q(\theta) \log \frac{1}{S} d\theta \quad (43)$$

Now the first term in Equation (43) is the KL-Divergence between two Mixture of Gaussians, which can be upper bounded using the same procedure as in [12], and the second term is a constant in the ELBO optimization. Therefore:

$$D_{KL}(q||\hat{p}(\cdot, t)) \leq D_{KL}(\chi^{(2)}||\chi^{(1)}) + \log \frac{1}{S} + \sum_{i,j} \chi_{j,i}^{(2)} D_{KL}(f_i^q||f_j^{\hat{p}}), \quad (44)$$

where we are rewriting $q = \sum_i c_i^q f_i^q$ and $\hat{p} = \sum_j c_j^{\hat{p}} f_j^{\hat{p}}$ with c_x^y being a generic weight and $f_x^y = \mathcal{N}(\mu_x^y, \Sigma_x^y)$ being a generic component, $(x, y) \in \{(i, q), (j, \hat{p})\}$. Furthermore, we have:

$$\chi_{i,j}^{(1)} = \frac{c_j^{\hat{p}} \chi_{j,i}^{(2)}}{\sum_{i'} \chi_{j,i'}^{(2)}}, \quad \chi_{j,i}^{(2)} = \frac{c_i^{(q)} \chi_{i,j}^{(1)} e^{-D_{KL}(f_i^q||f_j^{\hat{p}})}}{\sum_{j'} \chi_{i,j'}^{(1)} e^{-D_{KL}(f_i^q||f_{j'}^{\hat{p}})}}. \quad (45)$$

Finally, notice that $c_i^q = \frac{1}{C}$ for each i , where C is the number of components for the posterior, whereas $c_j^{\hat{p}} = \frac{1}{S a_0(-\rho)N\lambda} K_T(\frac{t-t_i}{\lambda})$, with a little abuse of notation over the index i and j .

C Proof of Theorem 4.1

The prof of Theorem 4.1 is straightforward, we just need to follow the same procedure of [37] plugging in the bound on the KL-Divergence of Equation 44. In the following we report the proof for completeness.

Proof. We start from Lemma 2 of [37] with variational parameter $\hat{\xi} = (\hat{\mu}_1, \dots, \hat{\mu}_C, \hat{\Sigma}_1, \dots, \hat{\Sigma}_C)$, whereas, for the right-hand side, we set $\mu_i = \theta^*$ and $\Sigma_i = cI$ for each $i = 1, \dots, C$, for some $c > 0$:

$$\begin{aligned} \mathbb{E}_{q_{\xi}} \left[\left\| \tilde{B}_{\theta} \right\|_{\nu}^2 \right] &\leq \inf_{\xi \in \Xi} \left\{ \mathbb{E}_{q_{\xi}} \left[\left\| \tilde{B}_{\theta} \right\|_{\nu}^2 \right] + \mathbb{E}_{q_{\xi}} [v(\theta)] + 2 \frac{\psi}{N} D_{KL}(q_{\xi}||\hat{p}) \right\} + 8 \frac{R_{max}^2}{(1-\gamma)^2} \sqrt{\frac{\log \frac{2}{\delta}}{2N}} \\ &\leq \mathbb{E}_{\mathcal{N}(\theta^*, cI)} \left[\left\| \tilde{B}_{\theta} \right\|_{\nu}^2 \right] + \mathbb{E}_{\mathcal{N}(\theta^*, cI)} [v(\theta)] + 2 \frac{\psi}{N} D_{KL}(\mathcal{N}(\theta^*, cI)||\hat{p}) + \\ &\quad 8 \frac{R_{max}^2}{(1-\gamma)^2} \sqrt{\frac{\log \frac{2}{\delta}}{2N}}. \end{aligned} \quad (46)$$

From Appendix B we have:

$$\begin{aligned} D_{KL}(\mathcal{N}(\theta^*, cI)||\hat{p}) &\leq \\ D_{KL}(\chi^{(2)}||\chi^{(1)}) + \log \frac{1}{S} + \sum_j \chi_j^{(2)} D_{KL}(\mathcal{N}(\theta^*, cI)||\mathcal{N}(\theta_j, \sigma^2 I)), \end{aligned} \quad (47)$$

where

$$\chi_j^{(1)} = c_j^{\hat{p}}, \quad \chi_j^{(2)} = \frac{c_j^{\hat{p}} e^{-D_{KL}(\mathcal{N}(\theta^*, cI)||\mathcal{N}(\theta_j, \sigma^2 I))}}{\sum_{j'} c_{j'}^{\hat{p}} e^{-D_{KL}(\mathcal{N}(\theta^*, cI)||\mathcal{N}(\theta_{j'}, \sigma^2 I))}} \quad (48)$$

obtained noticing that we can remove the index i because we have reduced the posterior to one component. $\chi_j^{(2)}$ can be rewritten:

$$\chi_j^{(2)} = \frac{c_j^{\hat{p}} e^{-\frac{1}{2\sigma^2} \|\theta^* - \theta_j\|}}{\sum_{j'} c_{j'}^{\hat{p}} e^{-\frac{1}{2\sigma^2} \|\theta^* - \theta_{j'}\|}} \quad (49)$$

if we plug in the closed form expression of the KL-Divergence (50) into its definition.

$$D_{KL}(\mathcal{N}(\theta^*, cI) \parallel \mathcal{N}(\theta_j, \sigma^2 I)) = \frac{1}{2} \left(p \log \frac{\sigma^2}{c} + p \frac{c}{\sigma^2} + \frac{\|\theta^* - \theta_j\|}{\sigma^2} - p \right). \quad (50)$$

Now we proceed upper bounding the first and then the third term of 47:

$$D_{KL}(\chi^{(2)} \parallel \chi^{(1)}) = \sum_j \chi_j^{(2)} \log \frac{\chi_j^{(2)}}{\chi_j^{(1)}} \quad (51)$$

$$= \sum_j \chi_j^{(2)} \log \chi_j^{(2)} - \sum_j \chi_j^{(2)} \log \chi_j^{(1)} \quad (52)$$

$$\leq \sum_j \chi_j^{(2)} \log \frac{1}{c_j^{\hat{p}}} \quad (53)$$

where we got 53 just noticing in 52 that the first term is negative. Considering the third term, we have:

$$\begin{aligned} \sum_j \chi_j^{(2)} D_{KL}(\mathcal{N}(\theta^*, cI) \parallel \mathcal{N}(\theta_j, \sigma^2 I)) &= \frac{1}{2} \sum_j \chi_j^{(2)} \left(p \log \frac{\sigma^2}{c} + p \frac{c}{\sigma^2} + \frac{\|\theta^* - \theta_j\|}{\sigma^2} - p \right) \\ &\leq \frac{1}{2} p \log \frac{\sigma^2}{c} + \frac{1}{2} p \frac{c}{\sigma^2} + \sum_j \chi_j^{(2)} \frac{\|\theta^* - \theta_j\|}{2\sigma^2}. \end{aligned} \quad (54)$$

Therefore:

$$\begin{aligned} D_{KL}(\mathcal{N}(\theta^*, cI) \parallel \hat{p}) &\leq \\ &\sum_j \chi_j^{(2)} \log \frac{1}{c_j^{\hat{p}}} + \log \frac{1}{S} + \frac{1}{2} p \log \frac{\sigma^2}{c} + \frac{1}{2} p \frac{c}{\sigma^2} + \sum_j \chi_j^{(2)} \frac{\|\theta^* - \theta_j\|}{2\sigma^2}. \end{aligned} \quad (55)$$

Now leveraging the above equation, the following upper bound obtained in the proof of Theorem 3 in [37]:

$$\mathbb{E}_{\mathcal{N}(\theta^*, cI)} \left[\left\| \tilde{B}_\theta \right\|_\nu^2 \right] \leq 2 \left\| \tilde{B}_{\theta^*} \right\|_\nu^2 + \frac{1}{2} \gamma^2 \kappa^2 c^2 \phi_{max}^4 + c(\theta_{max} \phi_{max} (1 + \gamma))^2, \quad (56)$$

and setting $c = \frac{1}{N}$ (since the bound hold for any constant parameter $c > 0$), $c_1 = \frac{8R_{max}^2}{\sqrt{2}(1-\gamma)^2}$, $c_2 = \theta_{max}^2 \phi_{max}^2 (1 - \gamma)^2 + \psi p \log \sigma^2 + 2\psi \sum_j \chi_j^{(2)} \log \frac{1}{c_j^{\hat{p}}} + 2\psi \log \frac{1}{S}$, $c_3 = \frac{1}{2} \gamma^2 \kappa^2 \phi_{max}^4 + \frac{\psi p}{\sigma^2}$ and $\varphi(\Theta_s) = \frac{1}{\sigma^2} \sum_j \chi_j^{(2)} \|\theta^* - \theta_j\|$, we can rewrite Equation (46) in the following way:

$$\mathbb{E}_{q_\xi} \left[\left\| \tilde{B}_\theta \right\|_\nu^2 \right] \leq 2 \left\| \tilde{B}_{\theta^*} \right\|_\nu^2 + v(\theta^*) + c_1 \sqrt{\frac{\log \frac{2}{\delta}}{N}} + \frac{c_2 + \psi p \log N + \psi \varphi(\Theta_s)}{N} + \frac{c_3}{N} \quad (57)$$

□

D Experimental Details

In this section, we provide some additional experimental details together with further results.

D.1 Parametrization

ADAM [16] is used in every experiment as optimizer. The source tasks are solved by a direct minimization of the TD error as described in section 3.4 of [37], using a *batch size* of 50 for the rooms environments and of 32 for Mountain Car, a *buffer size* of 50000, the projection parameter of the mellow-max TD error gradient set to 0.5, the learning rate $\alpha = 10^{-3}$. The exploration is ϵ -greedy with ϵ linearly decaying from 1 to 0.01 for Mountain Car and to 0.02 for the rooms environments. Both decays happen within 50% of the maximum number of learning iterations.

In the **rooms** environments, for what concern the two transfer algorithms, *c*-T2VT, and *c*-MGVT, we have the following parametrization: *batch size* of 50, *buffer size* of 50000, projection parameter of the mellow-max TD error gradient set to 0.5 (see section 3.4 of [37]), the parameter of Equation (2) $\psi = 10^{-6}$, 10 weights to estimate the expected TD error, the learning rates are set to $\alpha_\mu = 10^{-3}$ and $\alpha_L = 0.1$ for the mean and the Cholesky factor L of the posterior (moreover, the minimum eigenvalue reachable by L is set to $\sigma_{min}^2 = 10^{-4}$). Finally, for the prior, we use a diagonal isotropic matrix $H = 10^{-5}I$ and $\lambda = 0.3333$ in the context of *c*-T2VT, furthermore, we have $\Sigma = 10^{-5}I$ for the prior in the context of *c*-MGVT.

In the **Mountain Car** environment, *c*-T2VT and *c*-MGVT are parametrized in the following way: *batch size* of 500, *buffer size* of 10000, projection parameter of the mellow-max TD error gradient set to 0.5, the parameter of Equation (2) $\psi = 10^{-4}$, 10 weights to estimate the expected TD error, the learning rates are set to $\alpha_\mu = 10^{-3}$ and $\alpha_L = 10^{-4}$ for the mean and the Cholesky factor L of the posterior (moreover, the minimum eigenvalue reachable by L is set to $\sigma_{min}^2 = 10^{-4}$). Finally, for the prior, we use a diagonal isotropic matrix $H = 10^{-5}I$ and $\lambda = 0.3333$ in the context of *c*-T2VT, furthermore, we have $\Sigma = 10^{-5}I$ for the prior in the context of *c*-MGVT.

D.2 Temporal Dynamics

In this section, we provide the analytical form of the different dynamics employed in our experiments. Notice that these dynamics need to be plugged into the mean of our Gaussian distribution from where we sample the parametrization defining the task (for the rooms environment we will sample the positions of the doors, whereas, for the Mountain Car environment, we will sample the base speed).

- **Linear:** $2t - 1$, $t \in [0, 1]$;
- **Polynomial:** $at^4 + bt^3 + ct^2 + dt + e$, $t \in [0, 1]$ and $a = -15.625$, $b = 39.5833$, $c = -31.875$, $d = 9.91667$ and $e = -1$;
- **Sinusoidal:** $\sin(2\pi t)$, $t \in [0, 1]$.

In Figure 4, we report the graphical representation of the above analytical functions.

Now, given the range for a parameter $[k_{min}, k_{max}]$, a given dynamic will span over this interval in the following way: $d(t) \frac{(k_{max} - k_{min})}{2} + \frac{(k_{max} + k_{min})}{2}$. Finally, notice that, $[k_{min}, k_{max}] = [0.001, 0.0015]$ for Mountain Car, whereas $[k_{min}, k_{max}] = [0.7 + padding, 9.3 - padding]$ for the parameters of the rooms environments. The *padding* variable is 0 for the 2-rooms, whereas is 2 for the 3-rooms environments. This *padding* variable was necessary in the 3-rooms environments in order for the TD gradient algorithm to be able to solve the source tasks in every configuration of the two doors.

D.3 λ -sensitivity results

In Figures 5 and 6, we report a sensitivity analysis of our algorithm w.r.t. λ in the 2-rooms environment. This analysis is carried out computing the performance of the learning algorithm w.r.t. different values of the previously mentioned parameter (whereas $H = 10^{-5}I$ for every λ). These results are also compared with the performance of the algorithm when λ is chosen according to the likelihood optimization described in Section 6.5. In Figures 7 and 8, we report the above-described analysis in the context of the 3-rooms environment. In general, the performance of the likelihood approach is satisfying, for both 1-T2VT and 3-T2VT, even though in some cases it is not optimal. For what concern, the polynomial dynamic this may be due to its plateau (see Figure 4) which bias the choice for λ toward bigger values since the likelihood is evaluated in a cross-validation manner. For

the same reason, in the sin dynamic case, the likelihood-based approach tends to select an average λ . Finally, the linear case in the 2-rooms is almost optimal, whereas, in the 3-rooms, the performance decreases. This is due to the fact that, in the 3-rooms environment, we have 2 parameters governing the dynamics (the two doors positions) making the choice of λ harder to make in this setting.

Implementation Details: since the $\lambda \in [0, 1]$, we performed a grid search in order to optimize Equation 5 .

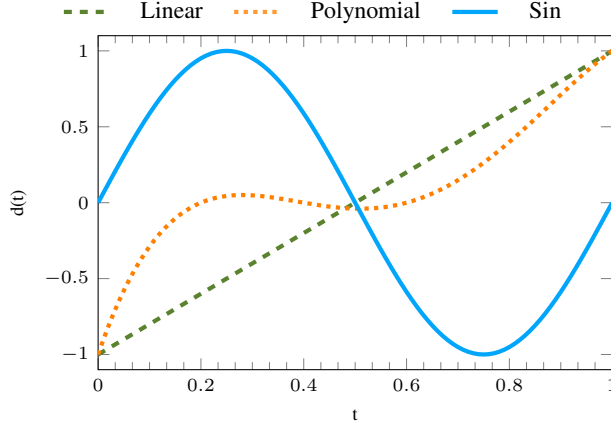
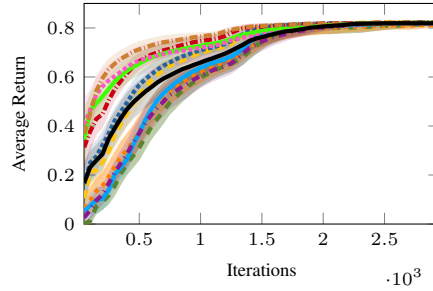


Figure 4: Temporal dynamics.



(a) 2-rooms polynomial dynamic.

(b) 2-rooms linear dynamic.



(c) 2-rooms sin dynamic.

Figure 5: Average return achieved by 1-T2VT w.r.t. different choices of λ with 95% confidence intervals computed using 50 independent runs.

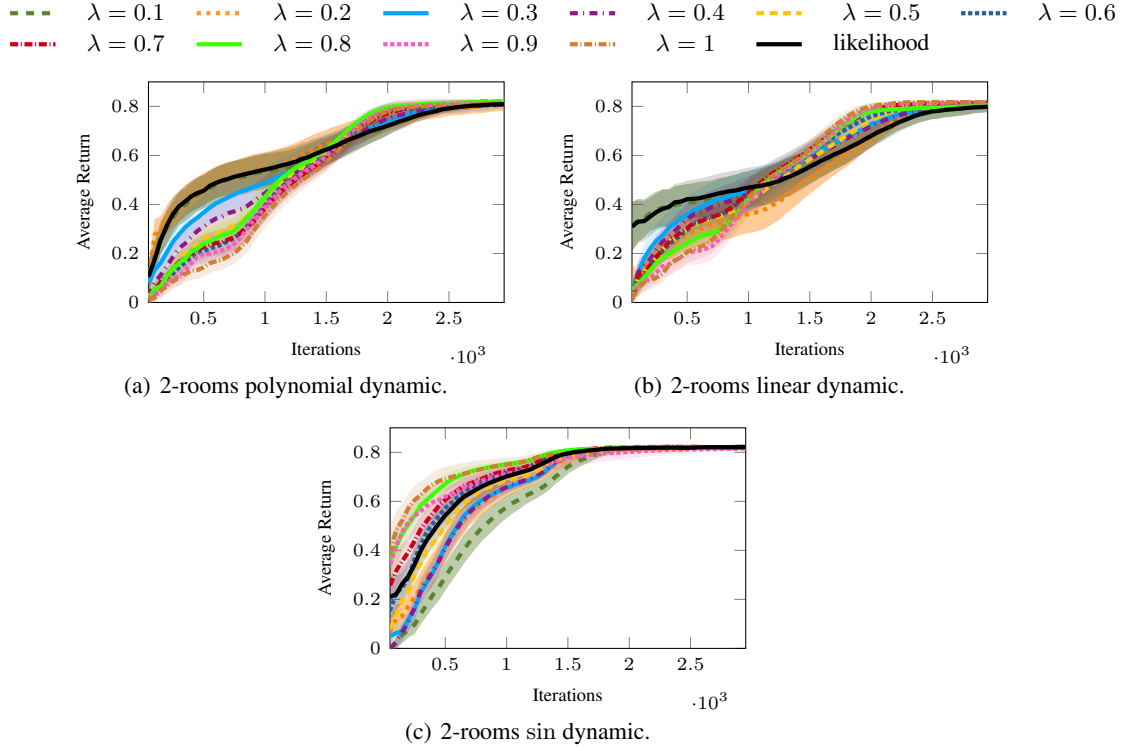


Figure 6: Average return achieved by 3-T2VT w.r.t. different choices of λ with 95% confidence intervals computed using 50 independent runs.

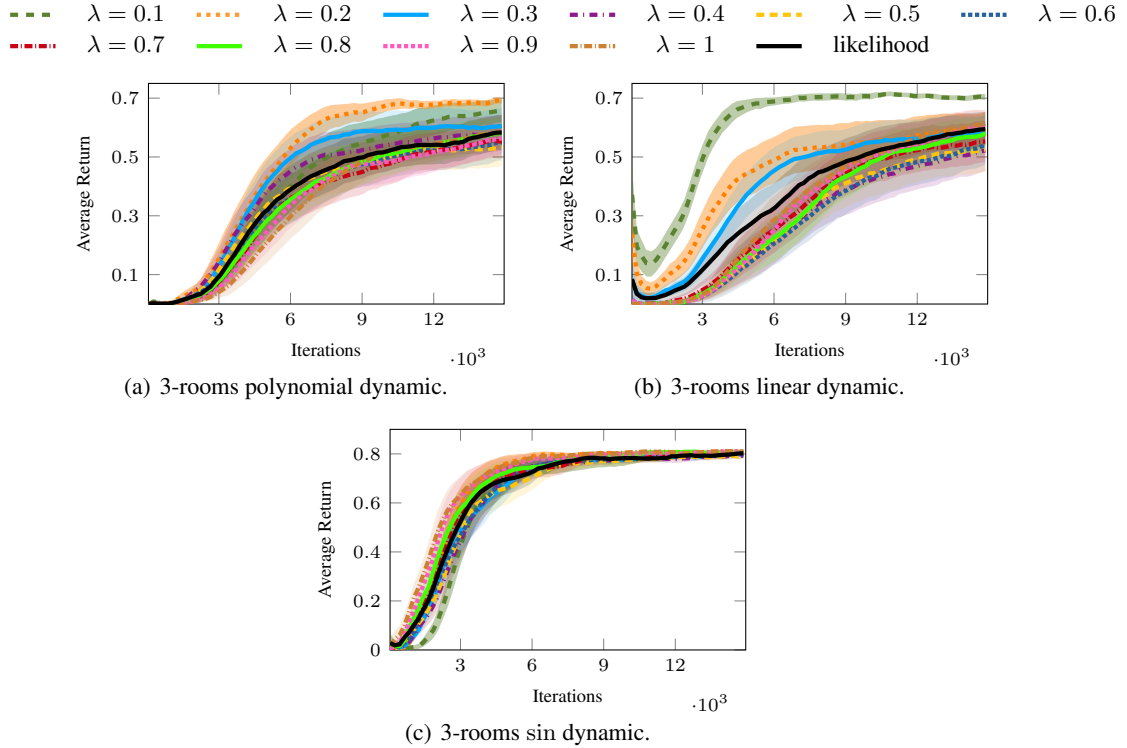


Figure 7: Average return achieved by 1-T2VT w.r.t. different choices of λ with 95% confidence intervals computed using 50 independent runs.

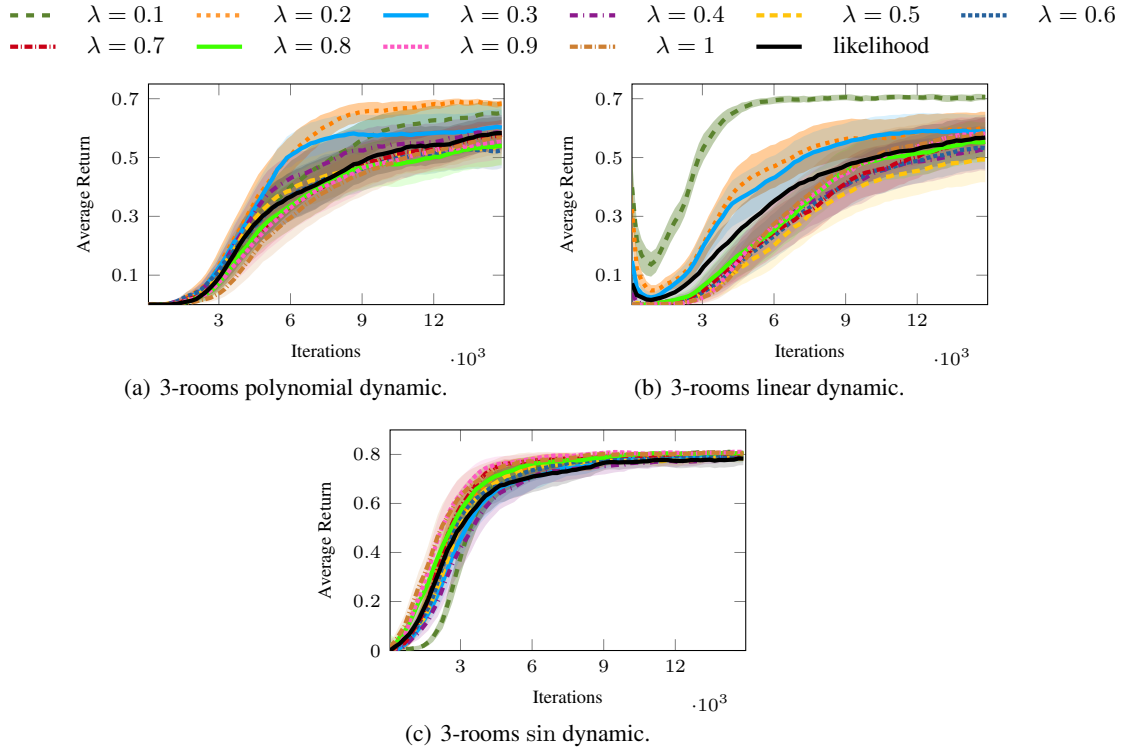


Figure 8: Average return achieved by 3-T2VT w.r.t. different choices of λ with 95% confidence intervals computed using 50 independent runs.